

SimTown: RF Propagation Models for Urban Femtocell Environments

Leonard Grokop, Chirag Patel, Mehmet Yavuz and Sanjiv Nanda
 {lgrokop, cpatel, myavuz, snanda}@qualcomm.com

ABSTRACT

Femtocells are miniature base stations (BS) improving cellular service typically within indoor environments such as homes or enterprise buildings. Analyzing femtocell performance and interference impact on the macro network requires the use of detailed RF propagation modeling, particularly in scenarios where user mobility is involved. This paper addresses this requirement by developing such models for urban neighborhoods using the WinProp® tool. Both femto and macro propagation are captured and the accuracy of the predictions is verified via field measurements. A detailed model of user mobility within the neighborhood is created. The utility of these models is demonstrated through an overview of two applications: mobile assisted range tuning for cdma2000 1xRTT beacon transmit power calibration, and a coverage analysis of open commercial femtocells versus distributed antenna systems.

1. INTRODUCTION

Femtocells are miniature base stations (BS) that are installed in a subscriber's residence or enterprise typically for improving cellular service within the indoor environment. Typically a femtocell is connected to the Internet and the cellular operator's network via a DSL router or cable modem. Key benefits of femtocells can be outlined as: excellent user experience indoors (through better coverage for voice and higher data throughput); offloading traffic load from macro cellular network and reduction of infrastructure deployment costs.

There are a number of potential interference issues that femtocells can suffer from due to unplanned deployments with low isolation between neighboring residences, and between residences and the street. Some of the issues relate to closed subscriber group (CSG) femtocells¹, which may cause interference to non-CSG users next door or outside. Refer to [1]-[2] for surveys of femtocells and different methods for interference management.

Many of these potential interference issues relate to mobility. For instance, if femtocell coverage extends too far, idle macro users passing on the street may attempt to register with a large number of femtocells each day, which may result in a reduction in handset standby-by time. Passing macro users in voice calls may be subjected to interference from the femtocell forward link and beacons² if they cannot perform active hand-in to the femtocell. If the passing user attempts active hand-in, it may experience difficulty resolving the ambiguity between neighboring femtocells due to the limited pool of scrambling codes used. If it does

perform active hand-in, voice artifacts may appear due to the hard nature of the hand-in. In order to assess the extent of these issues and to aid in designing and analyzing algorithms that mitigate them, RF propagation models that accurately capture the mobile behavior of users in femtocell environments are needed.

We have developed detailed three-dimensional path loss (PL) models for a number of urban femto environments using the WinProp® software tool developed by A.W.E. Communications [3]. Within the tool we utilize the dominant path prediction algorithm, which is a computationally efficient ray tracing feature that accounts for reflection, diffraction and penetration of electromagnetic waves off, around, and through media [4]. Using field measurements we have been able to demonstrate the validity and accuracy of the modeling software. The PL models developed incorporate both femtocell and macrocell signal propagation and give us the freedom to locate the environment anywhere in the macrocell. The models assume a carrier frequency of 2.0 GHz.

We concentrate on two key models in this paper:

- i) *Dense Urban Neighborhood (DUN)* – a model of a typical dense low to mid-rise residential apartment buildings in a city-like area,
- ii) *Suburban Neighborhood (SN)* – a model of a typical suburban neighborhood consisting of moderate sized two story houses with yards, trees, driveways, etc.

For each case we created a corresponding user mobility model by populating the neighborhood with hundreds of users of different types (residents, guests, automobiles, pedestrians) that go about their daily activities such as driving down the street, walking into a residence, moving around inside, etc. A PL and fading database was created for all users with 1.28s granularity, sampled continuously for 30 days. Location of each user in the neighborhood, times of voice activity, and user velocity are also recorded in the database. This model is useful in variety of simulations.

Additionally models were created for a number of other environments such as

- i) *Enterprise Campus* – a model of the Qualcomm campus, focusing on a specific building,
- ii) *Big Box Store* – a model of a big box retail store with aisles, checkout counters, etc...,
- iii) *Large House* – a model of a very large, three story, 6000 sq. ft. suburban home located in a woody area,

For the sake of brevity, we only present a brief discussion of the latter three models in this paper.

We start by giving an overview of the DUN and SN models in section 2. Section 3 demonstrates the accuracy of the models by comparison with field measurements. In section 4 we describe the macro and femto models in more detail. Section 5 details the user mobility model. Several applications of our models are presented

¹ CSG femtocells are those that restrict service to a limited subset of users, e.g. family members

² When the femtocell frequency is different from a neighboring macrocell frequency, a femtocell transmits a beacon (pilot plus overhead channels) to attract idle mobiles on the macrocell frequency to itself.

in section 6, exhibiting their utility. Section 7 briefly discusses the other models that have been created and conclusions are drawn in section 8.

2. OVERVIEW OF MODELING

With the A.W.E. software suite we primarily utilize two tools: WallMan and ProMan. WallMan is used to build a 3D model of the environment and select materials for each component from an extensive pre-tested material database. ProMan is used to run prediction simulations on the models designed in WallMan. For a given Tx antenna location and height, ProMan computes the PL to all Rx antenna locations on an X-Y grid of specified granularity, at specified heights. The software also has a database of sectorized antenna patterns that can be used in place of the default omni-directional antenna. We make use of this feature for macrocell propagation modeling.

In all simulations we use a 0.2x0.2m X-Y granularity for femto prediction, performing it over the entire neighborhood at street level, and at each floor level. Macro prediction must be conducted over a much larger area than femto, incorporating both the neighborhood and the macro BS located hundreds of meters away. However macro prediction is far less sensitive to geographic location than femto. For these reasons a coarser 0.6x0.6m granularity is used for macro prediction to speed up computation without sacrificing much detail.

2.1 Dense Urban Neighborhood

This is a model for a neighborhood of densely packed low to mid-rise wooden residential buildings with streets and pedestrian walkways separating the buildings. It consists of 8 apartment blocks, each approximately 20x50m and either 3 or 5 stories high. There are 10 apartments per floor, four of them having one bedroom (625 sq. ft.) and six of them having three bedrooms (1250 sq. ft.). Each apartment has a patio. The total number of apartments in the neighborhood is 320. The buildings are raised 0.5m from street level and each floor is 2.5m in height. The streets are 30-35m wide, the pedestrian walkways between the buildings are 10-15m wide. The neighborhood is approximately 200x200m and is surrounded by featureless concrete buildings of heights ranging from 5m to 11m, which act to diffract and reflect the macro signals that propagate into the neighborhood. A variety of materials from the WinProp® material catalogue are used for windows, internal dividers, internal walls, external walls, doors, furniture, floor/ceilings, plants and roof tiles. See Figure 1 and Figure 2.

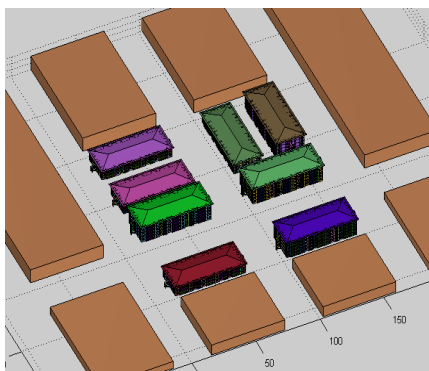


Figure 1: Dense Urban Neighborhood

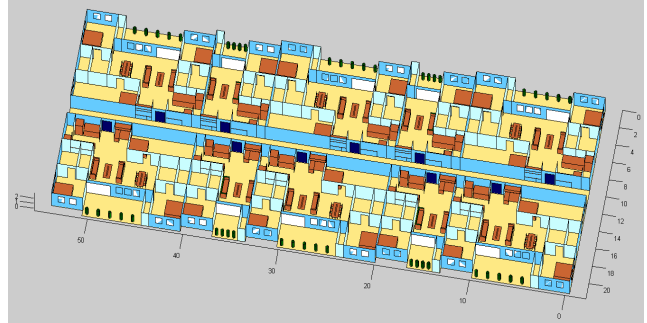


Figure 2: Floor plan of each building. There are 10 apartments per floor, each with either 1 or 3 bedrooms.

A sample path loss profile for a femtocell located inside one of the apartments, evaluated at a height of 2.1m above the street is shown in Figure 3. The dominant path prediction model is used with default settings except for LOS and OLOS PL exponents which are both set to 2.2, the NLOS value.

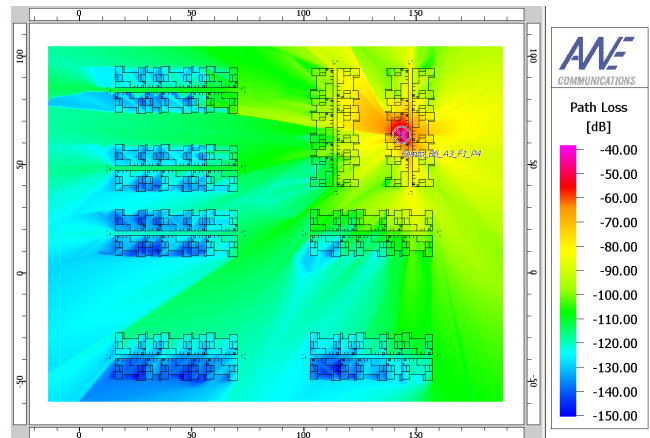


Figure 3: Sample path loss profile (bird's eye view) for a femtocell located in a 1st floor apartment

2.2 Suburban Neighborhood

This is a model for a typical suburban neighborhood consisting of 32 two-story, three bedroom houses and surrounding trees and plants in an area of approximately 200x200m. Together with the DUN model, the two models encompass the bulk of residential environments. Each home has about 2200 sq. ft of floor space, a two car garage, staircase, back and front yards, and resides on a 20x40m block of land. The streets are 10m wide. See Figure 4, and Figure 5 for renderings of the neighborhood.



Figure 4: Suburban neighborhood consisting of 32 houses

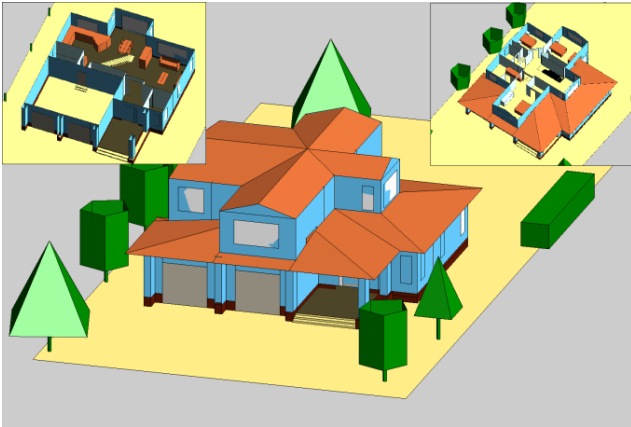


Figure 5: Suburban House. The 1st floor is shown in the top left. The 2nd floor is shown in the top right.

A sample path loss profile for a femtocell located on the 2nd floor of one of the houses, evaluated at a height of 1.6m above the ground is shown in Figure 6.

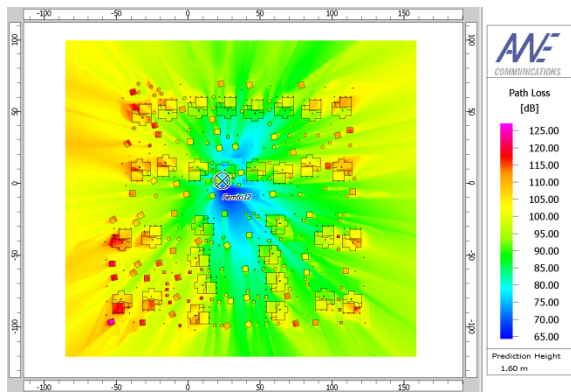


Figure 6: Sample path loss profile (bird's eye view) for a femtocell located on the 2nd floor of a house, evaluated at street level

3. MODEL ACCURACY

In order to verify that the PL predictions made by the RF propagation modeling software are accurate for the models constructed, field measurements made in neighboring apartments in a complex in San Diego were used. A photograph of the apartments is shown in Figure 7. Various measurements were made with transmitter and receiver in the same apartment, in neighboring apartments, and with transmitter inside and receiver outside. A model of this apartment setup was constructed in WinProp® (see Figure 8).



Figure 7: Apartments used in field measurements

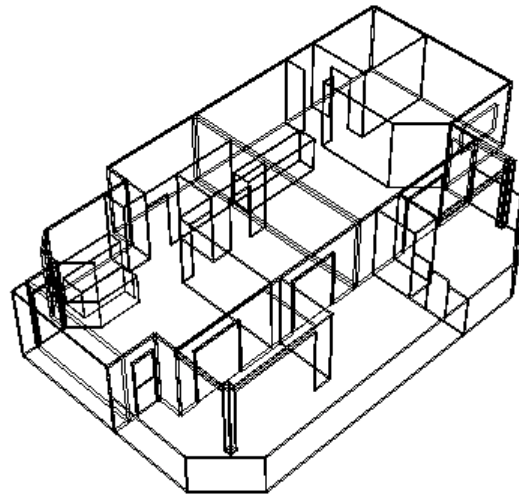


Figure 8: WinProp® replica model of apartment setup where field measurements were taken. Predictions were run using this model for comparison to field measurement data.

The WinProp® predictions and measurements for each Tx-Rx location are plotted in Figure 9. The standard deviation between predictions and measurements is 4.2dB, indicating good agreement. As the materials and construction used in the neighboring apartments model are identical to the materials and construction used in the DUN model, the conclusion is that the path loss predictions made inside and outside apartments in the DUN model have a standard deviation of 4.2dB, and are therefore reasonably accurate.

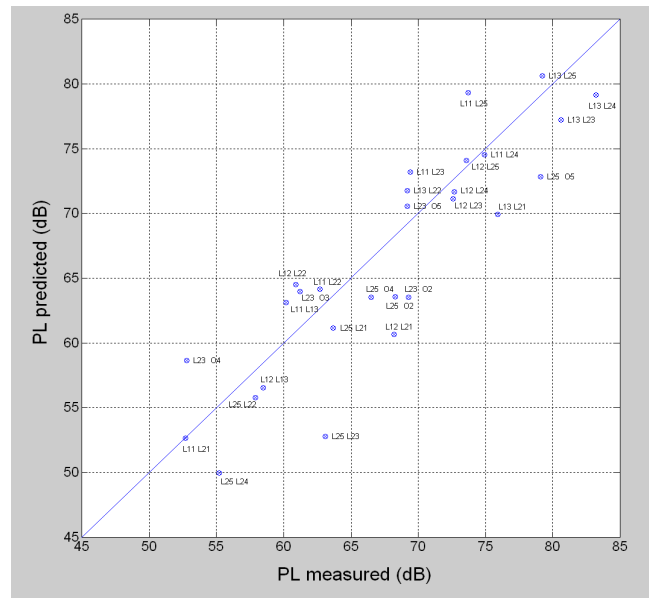


Figure 9: Comparison between WinProp® predictions and field measurements. The standard deviation between predictions and measurements is 4.2dB.

4. MODELING DETAILS

4.1 Macrocell propagation modeling

Macro signal strength is modeled for a range of locations of the neighborhood within the macrocell from cell center to cell edge. In order to do this without running the prediction tool exhaustively for each location, a single prediction is run with macro BSs in fixed positions and the resulting PL values offset by location dependent constants. These constants are computed based on a 57 macro sector honeycomb model. The same model is used for both the DUN and the SN.

In more detail, BSs A, B and C in the WinProp® model correspond to BSs 1, 9 and 8, respectively, in the honeycomb model. See Figure 10 and Figure 8. The equivalent figure to Figure 10 for the SN is omitted for brevity. BSs D and E in the WinProp® model are used solely to mimic the interference caused by the remaining 54 sectors in the honeycomb model. This is a slight approximation we make to make the computation more tractable.

Denote the PL generated by WinProp® BSs A-E at location (x,y,z) in the neighborhood by

$$PL_{WP,A}(x,y,z), \dots, PL_{WP,E}(x,y,z)$$

and the neighborhood center location used for calibration, by (x_c, y_c, z_c) . Denote the PL for the 57 macro sectors in the honeycomb model, evaluated at a particular neighborhood drop location (x_N, y_N) in the center cell by

$$PL_{HC,1}(x_N, y_N), \dots, PL_{HC,57}(x_N, y_N).$$

Then when the neighborhood is located such that its center is at (x_N, y_N) , we compute the path losses from macro BSs A-E to coordinate (x,y,z) as

$$\begin{aligned} PL_A(x,y,z,x_N,y_N) &= PL_{WP,A}(x,y,z) - PL_{WP,A}(x_c,y_c,z_c) \\ &\quad + PL_{HC,1}(x_N,y_N) \\ PL_B(x,y,z,x_N,y_N) &= PL_{WP,B}(x,y,z) - PL_{WP,B}(x_c,y_c,z_c) \\ &\quad + PL_{HC,9}(x_N,y_N) \\ PL_C(x,y,z,x_N,y_N) &= PL_{WP,C}(x,y,z) - PL_{WP,C}(x_c,y_c,z_c) \\ &\quad + PL_{HC,8}(x_N,y_N) \\ PL_D(x,y,z,x_N,y_N) &= PL_{WP,D}(x,y,z) - PL_{WP,D}(x_c,y_c,z_c) \\ &\quad - \frac{1}{2} \cdot 10 \log_{10} \left(\sum_{k \in \{1, \dots, 57\} \setminus \{1,8,9\}} 10^{-PL_{HC,k}(x_N,y_N)/10} \right) \\ PL_E(x,y,z,x_N,y_N) &= PL_{WP,E}(x,y,z) - PL_{WP,E}(x_c,y_c,z_c) \\ &\quad - \frac{1}{2} \cdot 10 \log_{10} \left(\sum_{k \in \{1, \dots, 57\} \setminus \{1,8,9\}} 10^{-PL_{HC,k}(x_N,y_N)/10} \right) \end{aligned}$$

Thus BSs D and E each account for half of the remaining interference.

To compute the PL for the honeycomb model we use standard 3GPP macro propagation model with 1km inter-site distance (ISD) for the DUN and 2km ISD for the SN. Shadowing is excluded as it is already captured by the WinProp® model.

Specifically, for the DUN model (1km ISD) we use

$$PL_{HC,k}(x_N, y_N) = 26.3 + 37.6 \log_{10}(d_k(x_N, y_N)) - G_{ant_pattern} + L_{add}$$

and for the SN model (2km ISD) we use

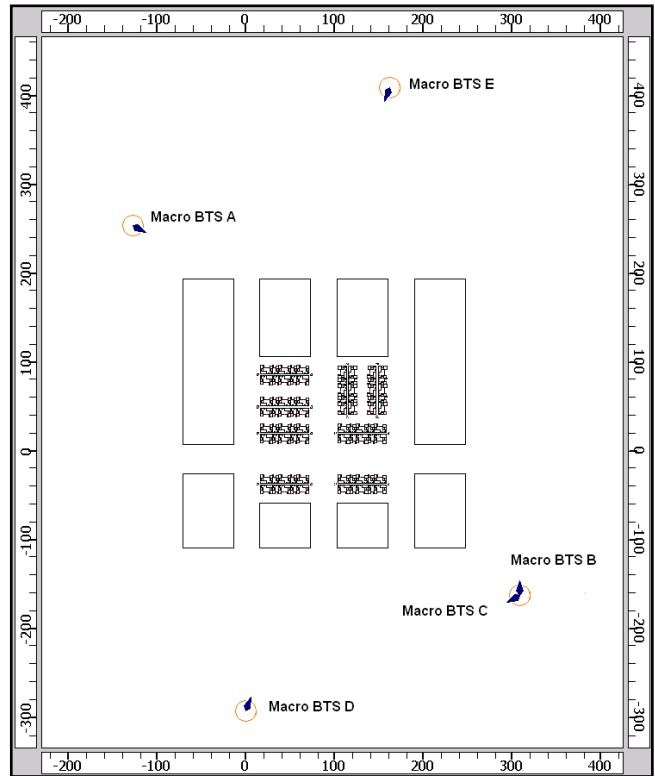
$$PL_{HC,k}(x_N, y_N) = 15.0 + 37.6 \log_{10}(d_k(x_N, y_N)) - G_{ant_pattern} + L_{add}$$

where

- $d_k(x_N, y_N)$ is the distance from macro BS k to coordinate (x_N, y_N) .
- $G_{ant_pattern}$ is the gain due to antenna pattern
- L_{add} consists of 14dBi macro antenna gain, 0dBi mobile antenna gain and 10dB other losses.

Note that both DUN and SN models produce the same *distribution* of values for $PL_{HC,k}(x_N, y_N)$.

Each WinProp® macrocell PL function $PL_{WP,A}(x,y,z)$ is computed on an (x,y) grid with 0.6m sampling, and evaluated at six heights for the DUN, $z = 1.6m$ (street level), $z = 2.1m$ (1st floor level), $z = 4.6m$ (2nd floor level), $z = 7.1m$ (3rd floor level), $z = 9.6m$ (4th floor level) and $z = 12.1m$ (5th floor level); and two heights for the SN, $z = 1.6m$ (street level/1st floor), $z = 4.6m$ (2nd floor). The heights correspond to the handset being located 1.6m above the floor.



(a)

Figure 10: Location of macro BSs in WinProp® model relative to the DUN. BSs D and E are used solely for generating out of cell interference

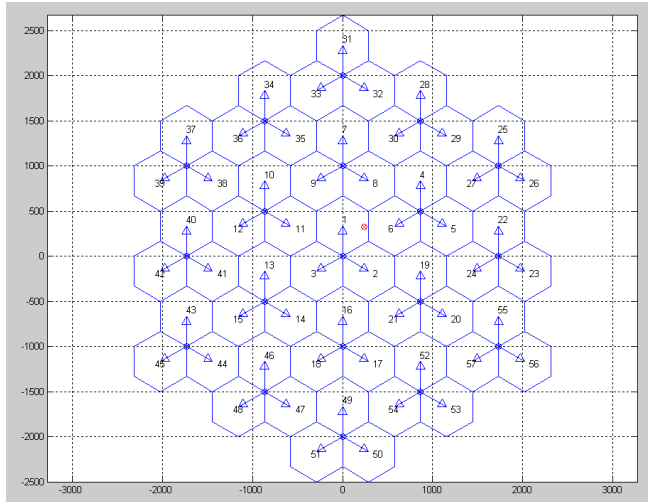


Figure 11: Macro honeycomb model with sectors labeled 1 – 57. A random neighborhood drop location in the center cell (cell #1) is shown in red. Honeycomb BSs 1, 8 & 9 are mapped to WinProp® BSs A, C & B, respectively.

4.1.1 Dense Urban Neighborhood

Figure 12 displays the PL distribution to the serving sector (i.e. the sector with the best forward link channel quality) in the DUN for the following three user classes:

- (a) users in apartments,
- (b) users in stairwells and corridors,
- (c) users outdoors.

All results are averaged over the 300 random drops of the neighborhood in the macrocell.

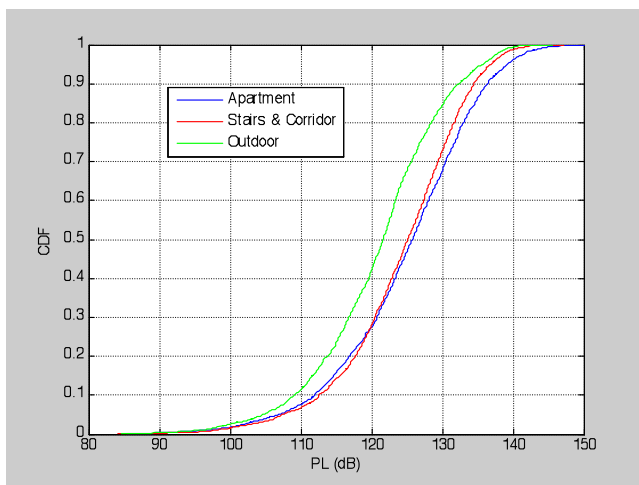


Figure 12: Path loss distributions for different user classes to the serving macro sector in the DUN

Figure 13 displays the 1xRTT I_o distribution for the same three user classes assuming an AT thermal noise power of -104dBm and 50% macrocell loading. Figure 14 shows the Ecp/Io distribution assuming Ecp/Ior = -7dB.

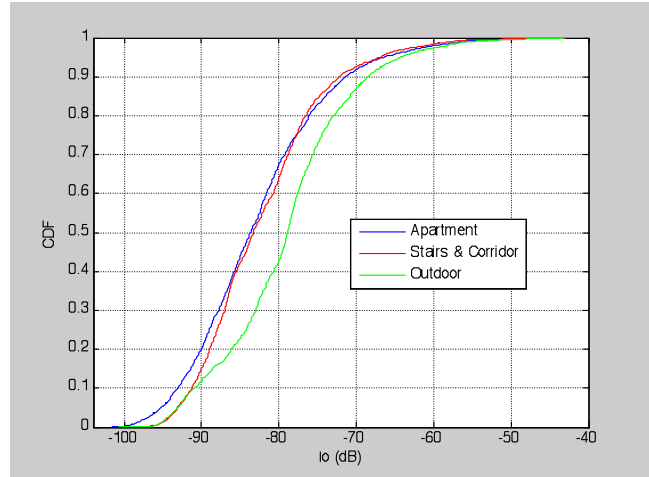


Figure 13: I_o distribution for 1xRTT users (macro only)

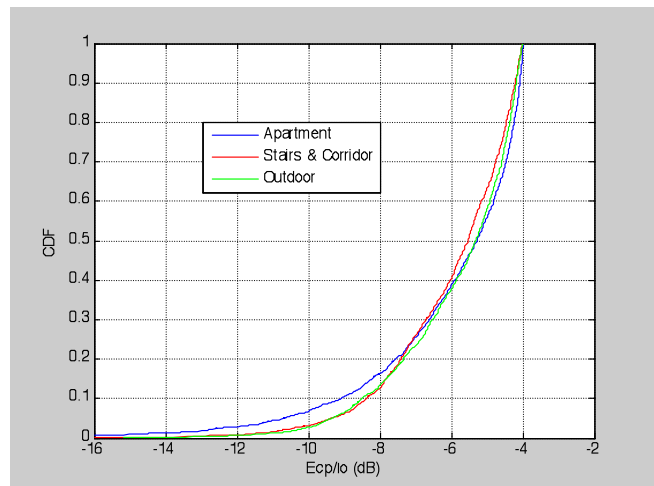


Figure 14: Macro Ecp/Io distributions for 1xRTT users

Figure 15 shows macrocell coverage for different building floors. Generally there is a monotonic increase in Ecp/Io with increasing height due to reduced macro signal penetration loss. Coverage is poorest on the first floor where 5% of apartments experience paging outage (Ecp/Io < -12dB). As the heights of the surrounding concrete buildings are no more than 11m, many of the 5th floor apartments (AT height 12.1m) have line of sight with the BSs. Consequently they experience superior coverage to the lower floors (<1% paging outage). Notice that the 2nd floor has slightly better coverage than the 3rd. This is due to the height of the surrounding buildings to the south. At 5m (2 stories) these buildings are tall enough to reflect the signal from macro A back into 2nd floor south facing apartments (height 4.6m), but not into 3rd floor south facing apartments (height 7.1m). This phenomenon showcases the level of detail of this RF propagation model.

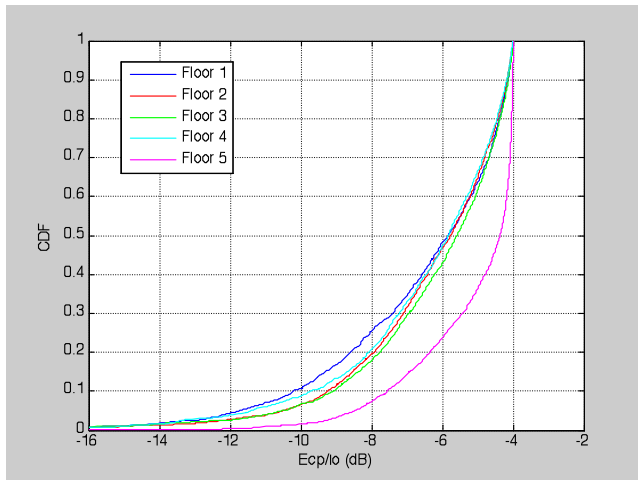


Figure 15: Macro Ecp/Io distributions on different floors.

4.1.2 Suburban Neighborhood

Figure 16 displays the path loss distribution to the serving sector in the DUN for the following three user classes:

- (a) users on first floor of house
- (b) users on second floor of house
- (c) users outdoors

All results are averaged over the 300 random drops of the neighborhood in the macrocell. Figure 17 and Figure 18 show the PL, 1xRTT Io and Ecp/Io distributions, respectively, assuming an AT thermal noise power of -104dBm, 50% macro loading and Ecp/Io = -7dB. There is little difference between first and second floor coverage, in fact first floor coverage is slightly better, due to a greater size and number of windows on the first floor (see Figure 5).

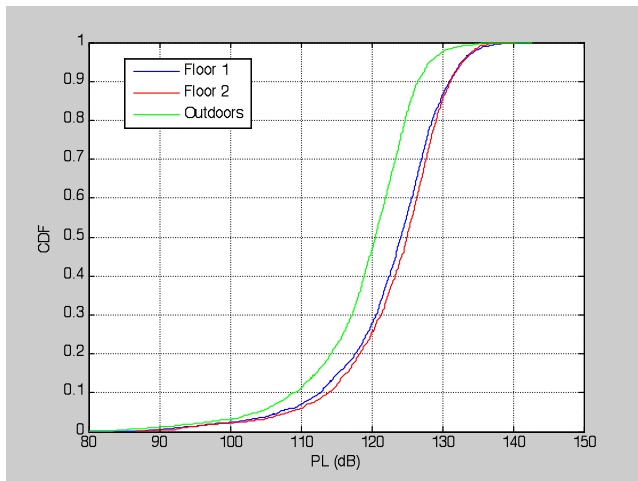


Figure 16: Path loss distributions for different user classes to the serving macro sector in the SN

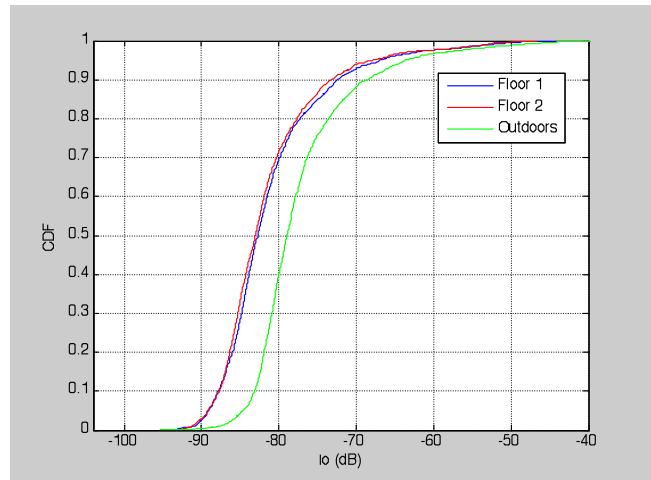


Figure 17: Io distribution for 1xRTT users (macro only)

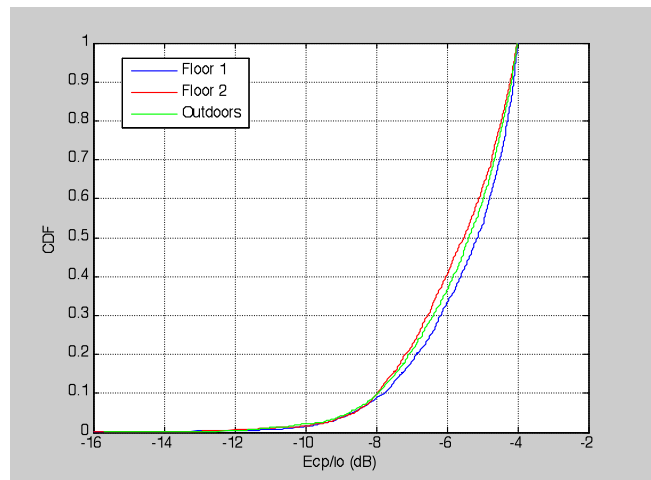


Figure 18: Macro Ecp/Io distributions for 1xRTT users

4.2 Femtocell propagation modeling

4.2.1 Dense Urban Neighborhood

Rather than computing path loss profiles for femtocells in all 320 apartments in the neighborhood, a computationally intensive exercise, we compute profiles only for a subset of 53 apartments. We bias the deployment of femtocells toward apartments with poorer coverage such that of the 53 for which path loss profiles are computed, 23 are located in 1st floor apartments, 12 in 2nd floor, 10 in 3rd floor, 3 in 4th floor and 5 in 5th floor. For each of these apartments, the femtocell is placed in 1 of 3 locations for the 1 bedroom apartment model and 1 of 5 locations for the 3 bedroom model. These locations are

1. On floor in living room behind sofa
2. On desk in living room
3. In bedroom 1, elevated 0.8m, and near window
4. In bedroom 2, elevated 0.8m (3 bedroom apartment only)
5. In bedroom 3, on floor near bedroom entrance (3 bedroom apartment only)

The locations of the 53 femtocells are shown from a bird's eye perspective in Figure 19. Note that a few femtocells are located directly below others and are hence not visible in this plot.

For various applications we down-sample this subset of femtocells to achieve lower penetration densities. The down-sampling is often done based on the coverage (macro E_{cp}/I_o) in individual apartments, apartments with poor macro coverage being more likely to have a femtocell.

Each WinProp® femtocell path loss function $PL_{WP,X}(x,y,z)$ is computed on an (x,y) grid with 0.2m sampling, and evaluated at the same heights as the macro propagation model.



Figure 19: Bird's eye view of DUN showing femto locations

Figure 20 shows the distribution of path loss to the strongest femtocell, for four different types of users – those

1. in an apartment with a femtocell (magenta)
2. in an apartment without a femtocell (blue)
3. in a corridor (red)
4. outdoors (green).

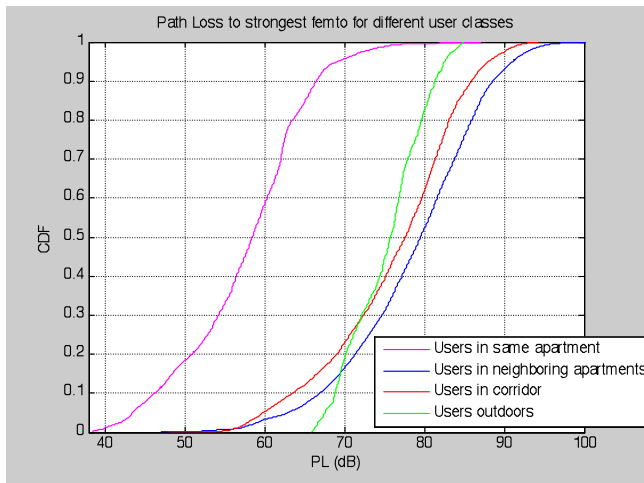


Figure 20: Distribution of path loss to strongest femtocell for different types of users in the DUN

4.2.1 Suburban Neighborhood

In the suburban neighborhood each of the 32 houses has a femtocell PL profile computed. Femtocells are deployed in one of six random locations

1. On kitchen countertop

2. In living room behind sofa
3. Near the door leading down into the garage
4. Upstairs in bedroom 1 on nightstand
5. Upstairs in bedroom 2 on nightstand
6. Upstairs in bedroom 3 on nightstand

These locations are illustrated in Figure 21.

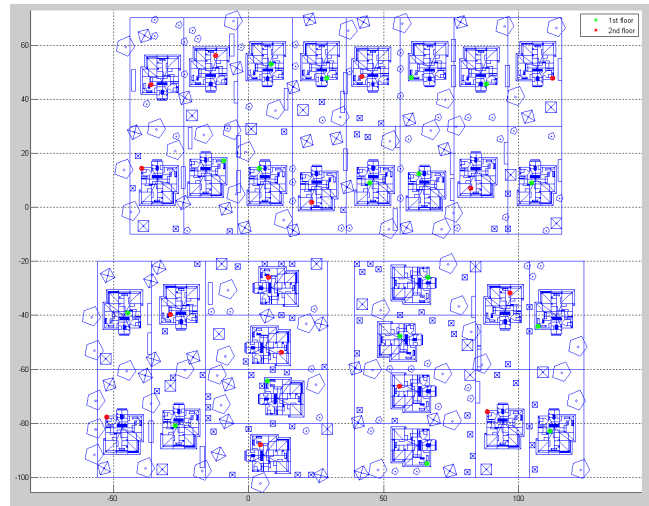


Figure 21: Bird's eye view of SN showing femto locations

Figure 22 shows the distribution of path loss between

1. an indoor user and the femto in the same house (blue)
2. an indoor user and the strongest femto in a neighboring house (red)
3. outdoor user and the strongest femto (green)

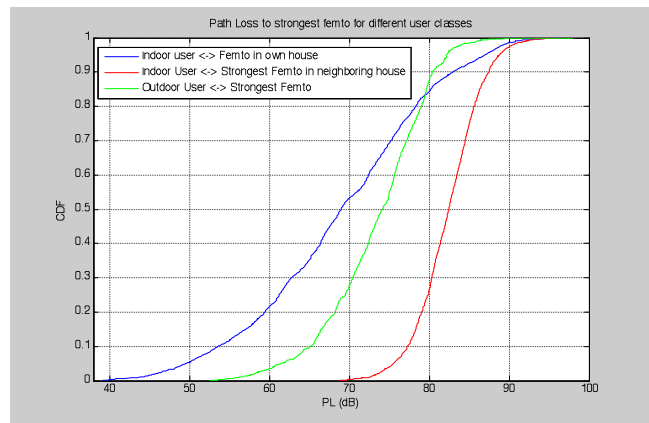


Figure 22: Distribution of path loss for different types of users in the SN

5. USER MOBILITY MODEL

So far we have described how PL is computed from each macro and femto basestation, to a given user location in the either the DUN or SN. This is sufficient for performing static analysis such as estimating the size of the outage region (“coverage hole”) created by a co-channel femto or a femto beacon transmitted on a macro carrier. It is also enables us to perform dynamic analysis on individual mobile users, for instance, finding the average time taken for an idle user returning home from work to find (i.e.

reselect to) its femto. However there are applications that require the neighborhood be populated with mobile users so that aggregate statistics can be computed for different algorithm designs. For example: counting the number of registrations femtocells receive each day (used for designing registration based power calibration algorithms). As such, we created a detailed mobility model that captures the behavior of mobile users going about their daily activity.

There are four types of users in both DUN and SN mobility models. These categories capture the bulk of people that typically visit, pass through, or reside in such a neighborhood.

1. *Apartment/Home users* – these users live in the neighborhood. Some leave for work each day and return in the evening, others stay at home, going out for shorter periods of the day.
2. *Guest users* – these users visit the apartment/home users on a sporadic basis. They stay for variable amounts of time and sometimes turn up in groups. Occasionally parties and large gatherings are held where many guest users visit a single residence in short period of time.
3. *Automobile users* – these users drive through the neighborhood at various speeds, sometimes stopping at traffic lights for a while, but not visiting any of the residences.
4. *Pedestrian users* – these users walk along the footpaths across the neighborhood, sometimes waiting at intersections to cross, but not visiting any of the residences.

We generate a database, where for each user the following mobility information is stored sampled every 1.28 sec (corresponding to a MS wake-up of every 1.28s) continuously for 30 days (24 hours per day).

- User location in neighborhood, i.e. (x,y,z) coordinates
- PL to each of the 53 femto and 5 macro BSs
- User velocity (0 if at rest)
- Call status (1 if the user is active, 0 otherwise)

For many samples, certain users are not present in the neighborhood, either because they are out, at work, yet to enter or pass through the neighborhood, etc... For these samples we treat PL to all cells as infinite.

5.1 Call Status

Call status is modeled in the following way. All users in the neighborhood switch between “idle” and “active” states according to a Markov chain with a transition probability matrix that depends upon the time of day.

Night: (12-6am)

$$\begin{bmatrix} \Pr(\text{idle} \rightarrow \text{idle}) & \Pr(\text{active} \rightarrow \text{idle}) \\ \Pr(\text{idle} \rightarrow \text{active}) & \Pr(\text{active} \rightarrow \text{active}) \end{bmatrix} = \begin{bmatrix} 0.99999 & 0.01 \\ 0.00001 & 0.99 \end{bmatrix}$$

Day Off Peak: (6-9am)

$$\begin{bmatrix} \Pr(\text{idle} \rightarrow \text{idle}) & \Pr(\text{active} \rightarrow \text{idle}) \\ \Pr(\text{idle} \rightarrow \text{active}) & \Pr(\text{active} \rightarrow \text{active}) \end{bmatrix} = \begin{bmatrix} 0.9999 & 0.01 \\ 0.0001 & 0.99 \end{bmatrix}$$

Day Peak: (9-5am)

$$\begin{bmatrix} \Pr(\text{idle} \rightarrow \text{idle}) & \Pr(\text{active} \rightarrow \text{idle}) \\ \Pr(\text{idle} \rightarrow \text{active}) & \Pr(\text{active} \rightarrow \text{active}) \end{bmatrix} = \begin{bmatrix} 0.9998 & 0.01 \\ 0.0002 & 0.99 \end{bmatrix}$$

Evening Peak: (5-9pm)

$$\begin{bmatrix} \Pr(\text{idle} \rightarrow \text{idle}) & \Pr(\text{active} \rightarrow \text{idle}) \\ \Pr(\text{idle} \rightarrow \text{active}) & \Pr(\text{active} \rightarrow \text{active}) \end{bmatrix} = \begin{bmatrix} 0.9996 & 0.01 \\ 0.0004 & 0.99 \end{bmatrix}$$

Evening Off Peak: (9pm-12am)

$$\begin{bmatrix} \Pr(\text{idle} \rightarrow \text{idle}) & \Pr(\text{active} \rightarrow \text{idle}) \\ \Pr(\text{idle} \rightarrow \text{active}) & \Pr(\text{active} \rightarrow \text{active}) \end{bmatrix} = \begin{bmatrix} 0.9999 & 0.01 \\ 0.0001 & 0.99 \end{bmatrix}$$

Thus the average call lasts $(1-0.01)/0.01 * 1.28 = 126.7$ seconds and each user is active for an average of 694.5 minutes per month.

We now describe the mobility model used for each class in more detail.

5.2 Dense Urban Neighborhood

We assume 80% wireless penetration and 30% operator share, so that 24% of all people in the neighborhood are users on a given operators network.

5.2.1 Apartment users

These users live in apartments in the DUN. Each 1 bedroom apartment contains one user with a 24% chance, each 3 bedroom apartment contains a family of three with 50% chance, in which case there is a 24% chance that all three of these occupants are users, and contains individual occupants with 50% chance, in which each of them independently has a 24% chance of being a user.

Each user independently either goes to work (80% chance) or stays at home (20% chance).

Users that go to work/school each day wake at a random time uniform from 6-8am, leaving their apartment 0.5-1 hour later, and returning 8-11 hours later. The same wake, leave, and return times are used for a given user for the entire 30 day period. There is a 50% chance, independent from day to day, that upon returning from work, the user will go out again 0.5-1 hours later and return 1-2 hours after this, and then go to bed at a random time between returning home and 11:45pm. There is a 50% chance, independent from day to day, that upon returning from work, the user will not leave the apartment again that day, and go to bed at a random time between 10 and 11:45pm.

Users that do not go to work/school wake at a random time uniform from 7-10am, leave the apartment at a random time 0.5-6 hours later, returning 1-4 hours after this. With a 50% chance the non-working user leaves for a second time 0.5-1 hours after returning from the first outing, and stays out for 1-2 hours before returning for the second time, going to bed at a random time between the second return and 11:45pm. With 50% chance the non-working user does not go out for a second time. All non-working user departure and return times are independent from day to day.

When users return home they reappear in the neighborhood at the bottom of the stairs of their apartment building (we assume they park beneath the building). They then walk up the stairs to their floor, along the corridor to the door of their apartment, and enter. We refer to this as the *approach* route. After entering their apartment they move along the *apartment circuit* route in a manner described below. An example of these routes is given in

Figure 23 and Figure 24. When a user leaves its apartment, it simply uses the reverse of its approach route.

Additionally, each user is classified as either a *handset carrier* (20% chance) or a *non handset carrier* (80% chance).

Handset carriers keep their handsets in their pockets all day, taking them out only for calls, and when they go to bed, in which case the handset is placed on the nightstand next to their bed. When a handset carrier returns home, it begins to move at 3km/h along the apartment circuit route according to a Markov model with 2 states, “moving” and “stationary”. Each 1.28 sec sample, users transition between these states according to the following transition probability matrix:

$$\begin{bmatrix} \Pr(sta \rightarrow sta) & \Pr(mov \rightarrow sta) \\ \Pr(sta \rightarrow mov) & \Pr(mov \rightarrow mov) \end{bmatrix} = \begin{bmatrix} 0.9992 & 0.1 \\ 0.0008 & 0.9 \end{bmatrix} \quad (1)$$

When handset carriers place or receive calls, they simultaneously transition to the moving state (if not already in this state) and start walking.

Non-handset carriers upon returning to their apartments always walk at 3km/h to one of six resting locations and place their handsets there. The resting location is chosen independently from day to day (in contrast to handset carriers). They only return to these locations to place or receive a call.

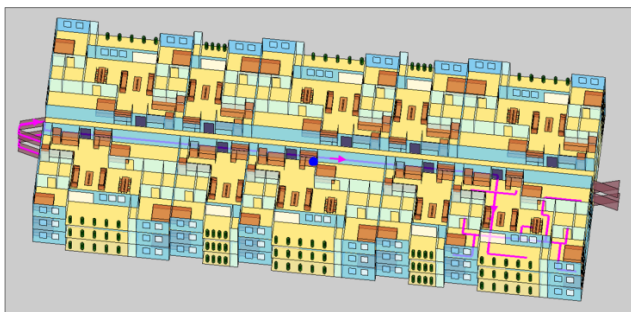


Figure 23: Apartment approach route and circuit route drawn in magenta, for a user residing in the bottom right apartment on the third floor of the building.



Figure 24: Circuit route for three bedroom apartment.

5.2.2 Guest users

Guest users are those that visit apartments but do not live there, such as friends, relatives, maintenance staff, etc.... Each apartment

i has a random *group visitation intensity* G_i which has an exponential distribution with mean

$$E(G_i) = 0.24 * num_bedrooms / 7 / 10.75 / 3600 * 1.28.$$

The group visitation intensity dictates how frequently an apartment will be visited by groups of guest users. Every 1.28s between the hours of 10am and 8:45pm a group of guest users arrives at apartment *i* with probability G_i . The group stays for 1-3 hours. Note that guests can potentially visit all apartments in the neighborhood, not just those that contain a resident on the operators network. The number of guests in each group is geometrically distributed with mean $N = 1.2$, independent from group to group. All guests belong to the operators network, that is, we don't need to model non-user guests. Thus the average number of visitors (including non-users) apartment *i* experiences per day is approximately

$$NG_i * 3600 / 1.28 * 10.75 / 0.24,$$

and the number of visitors per day averaged over both days and apartments is approximately

$$N * num_bedrooms / 7.$$

That is, the average bedroom is visited by one group of guests per week.

Additionally, for each day and apartment, there is 1% chance a party is held. If a party is held, it starts sometime between 12pm and 6pm. For the next 2 hours guest users show up at the apartment with 500 times the regular visitation intensity. Each partygoer stays for 1-3 hours.

After entering the apartment each guest user proceeds to walk along the apartment circuit route according to the 2 state Markov model with transition probability matrix given by equation (1).

5.2.3 Automobile users

These users drive through the neighborhood but do not live in it. All automobile users add 6dB PL to all signals to account for car penetration loss. There are 6 automobile routes, one for each lane of the two main streets in the neighborhood. These routes are highlighted in blue in Figure 25 and their directions are indicated with arrows. Cars arrive at the start of each route according to a Poisson process with mean number of cars per hour given in the Table 1.

Time of day	E[cars per lane per hour]
10pm-7am	20
7-9am	300
9am-12pm	100
12-1pm	300
1-4pm	100
4-7pm	300
7-10pm	100

Table 1: Traffic intensity by time of day

Note that only 24% of these cars (independently chosen) are users on the operators network. The reason we model all cars is to correctly capture traffic behavior.

Drivers move straight along their route, without turning, though there is an intersection in the center of the neighborhood with traffic lights where they sometimes stop. See Figure 25. The

traffic lights at the intersection alternate between red and green every minute with 50% duty cycle. The last 5×1.28 seconds of the green period corresponds to orange. Each car sets its velocity according to the distance to the car in front it d , and its velocity v , so as to be able to break in time in order to avoid coming within a distance s of them, given a maximum braking deceleration of b and a reaction time of r . Velocity is also limited according to the lane in which the car is driving. The formula for setting velocity v' of a car is given by equation (2).

$$v' = \min \left(v_{\max}, \sqrt{rb + 2(d-s)b + v^2 - rb} \right) \quad (2)$$

The maximum velocity for the inner lanes of the left-right routes of Figure 25 is 36mph. For the outer lanes it is 29mph. For top-bottom lanes it is 25mph.

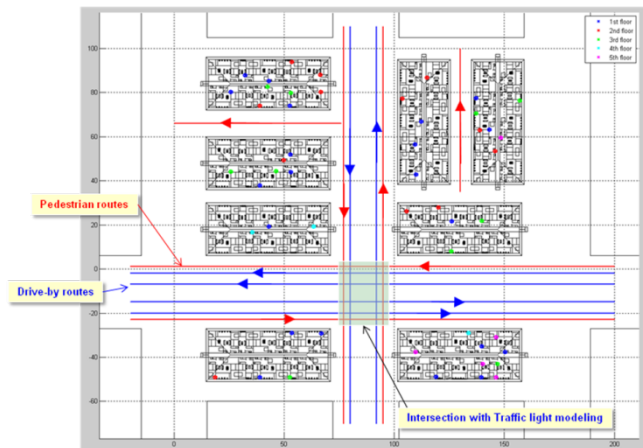


Figure 25: Automobile and Pedestrian routes

For a given route, each time the traffic light turns orange, a *lead car* is determined. This is the first car that will stop at the light. All cars ahead of the lead have determined that they will not be able to break in time. The lead car is able to break in time and sets its velocity according to equation (2), treating the intersection as a stationary car. Consecutively one by one, each car behind the lead slows down accordingly, each calculating their velocity according to the distance to, and velocity of the car in front. Figure 26 shows an example of how the intersection affects traffic during rush hour.

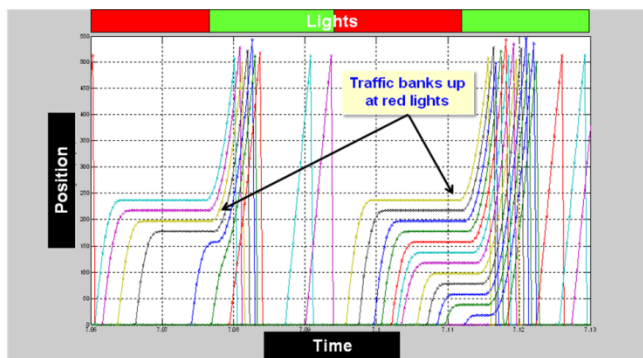


Figure 26: Traffic during rush hour

The inclusion of intersection behavior in our model may at first glance seem unnecessarily detailed, however many applications are sensitive to a cars velocity, and whether or not it stops at an intersection. For instance, a car driving at high velocity is unlikely

to register with a femtocell that it passes, whereas a car stopped in traffic will likely do so.

5.2.4 Pedestrian users

There are 6 routes of pedestrian traffic, 4 footpath routes (alongside streets) and 2 walkways between buildings. See Figure 25. Pedestrian routes are highlighted in red. Footpath traffic is treated similarly to automobile traffic. The arrival intensity during different hours of the day is set to 1/10 of the automobile values given in Table 1. Maximum velocity is 3.6km/h. For pedestrian traffic we only model users on the operators network. Thus the arrival intensity of pedestrian users is $1/10 \times 0.24 = 0.024$ of the values in Table 1. For a user walking down the footpath, a graph showing PL to the 53 femtocells in the neighborhood as a function of time is given in Figure 27.

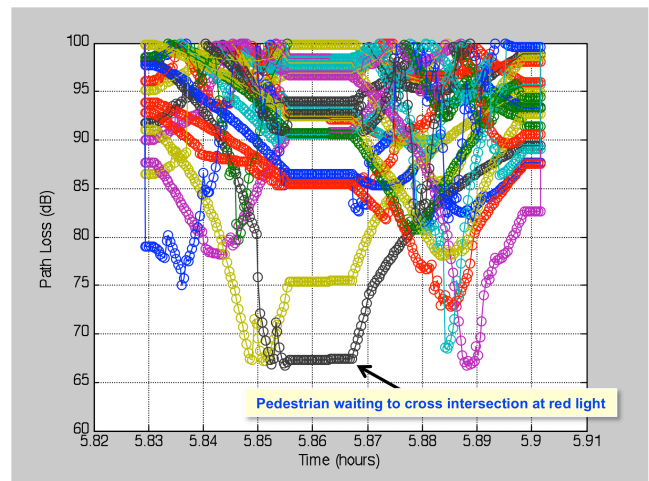


Figure 27: PL as a function of time, for pedestrian walking down footpath to 53 femtos in the neighborhood.

5.3 Suburban Neighborhood

The user mobile mobility for the SN is very similar to the DUN. The same four user types exist and behave in a similar fashion. We give a brief overview of the differences. When returning home a house user drives down the street, into its driveway and garage, and then gets out of the car and walks to the garage door entrance to the house. The reverse route is taken when leaving. Whilst inside their cars, house users experience 6dB greater PL to all cells, due to car penetration loss. Examples of these routes are given in Figure 28. The house circuit route is shown in Figure 29. Each house is occupied by a family with probability 0.9 (c.f. 0.5 in the DUN) and the number of people per house is uniform from 1-5. Guest users approach the house by car, then park in the driveway, walk to the front door and wait 10×1.28 seconds for it to be opened, before entering. No intersections are modeled in the suburban model, and automobile users drive straight through the neighborhood at 25mph, along 1 of 3 streets. Automobile arrival intensities are 1/10 the values that they take on in the DUN. Pedestrian users walk the same routes with 1/3 the automobile arrival intensity. Due to the sparsity of users in the SN, 5 independent datasets are generated for the user mobility model and results are averaged.

5.4 Fading

To all PL traces generated by the user mobility models, we add fading. A single-path Rician fading simulator with $K = 1.5$ (linear)

is used for femto signals and $K = 5$ is used for macro signals. These values are based on field measurements. Note that although in practice the macro signal often consists of multiple paths, for our purposes it suffices to simply model the combined effect as a single-path. The choice of these values is based on an extensive measurement campaign. The simulator takes into account the velocity of the user.



Figure 28: Approach routes for house users in the SN



Figure 29: House circuit route

6. APPLICATIONS

In this section we give an overview of various applications of the DUN and SN models and the corresponding user mobility models.

6.1 Mobile assisted range tuning

When a femtocell is deployed on a dedicated 1xRTT carrier it is common for beacons to be transmitted on macro carriers to enable users to discover it. The beacon consists of the pilot, paging and synchronization channels. When an idle user enters the vicinity of a beacon it reselects to it and is subsequently sent a redirection message instructing it to search for the femtocell on a particular carrier and PN. In this manner femtocell discovery is facilitated.

One potential issue with this approach is spillover, i.e. RF interference caused by the femtocell beacon to nearby macrocell mobiles. If the femtocell has restricted access, we would like to limit the beacon range so that it does not leak outside the

apartment or home. Even if the femtocell has open access, if the beacon Tx power is too high, active users outside will experience FL voice artifacts as they walk or drive by. To mitigate this effect the beacon power is calibrated. Note that this does not preclude a dedicated femto from transmitting at high power (higher than beacon) in order to provide the users that have already discovered it with a large coverage area.

The simplest form of calibration is called *network listen power calibration* (NLPC) [6] where the femtocell measures the macro signal strength on a particular carrier and sets the beacon transmit power on that carrier so as to cover a radius of PL_{edge} dB. This calibrated setting sometimes underestimates or overestimates the required Tx power level. For example, if the femtocell is placed near a window, NLPC will yield a high value of E_{cp} , and hence a high power setting will be used, but this will be detrimental if there are many users outside.

To fine tune the power setting we use an approach called *Mobile Assisted Range Tuning* (MART), where at the end of each day the femtocell counts the number of unique registrations it has received and steps up or down its NLPC based power setting to regulate this quantity. In the case of signaling access or restricted access femtocells, the approach can be modified to incorporate home user measurements into the power tuning. In this section we assume open access femtos, i.e. any mobile user can be served.

The performance of the MART algorithm is simulated for both DUN and SN models. We assume users are uniformly distributed across 4 macro 1xRTT carriers and simulate a sparse hopping beacon that is present on each carrier for a few seconds each minute. Thus only users that are within beacon range when it is transmitted on their carrier, can potentially register. The same beacon Tx power setting is used for all 4 macro carriers.

The neighborhoods are populated with mobile users according to the user mobility models described in section 5. At the end of each day registrations are counted and the beacon Tx power is incrementally adjusted. Simulations are run for 14 continuous days.

For the DUN we simulate a deployment of 14 femtocells in the neighborhood, 7 of which are situated in 1st floor apartments, 1 in a 2nd floor, 5 in 3rd floor, and 1 in a 5th floor. The neighborhood is dropped at the *cell corner* location of the macrocell, illustrated in Figure 31.

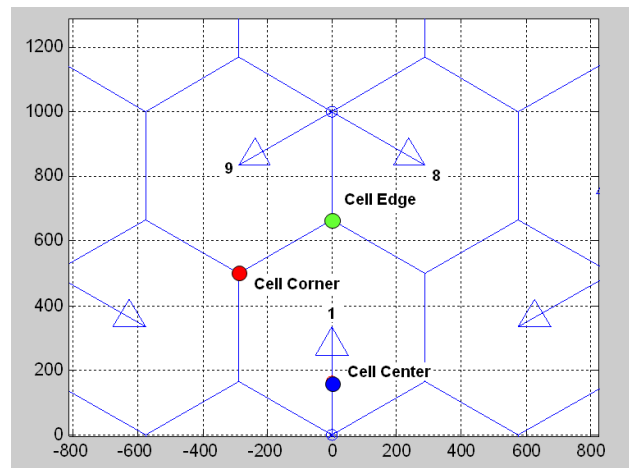


Figure 30: Cell center, cell edge, and cell corner drop locations for the neighborhood

The initial NLPC beacon Tx power values are displayed in Figure 31 along with the final values arrived at after 14 daily MART iterations. A value of 75dB is used for the PL_{edge} parameter, and $E_{cp/Ior} = -3dB$, when computing the initial NLPC power values.

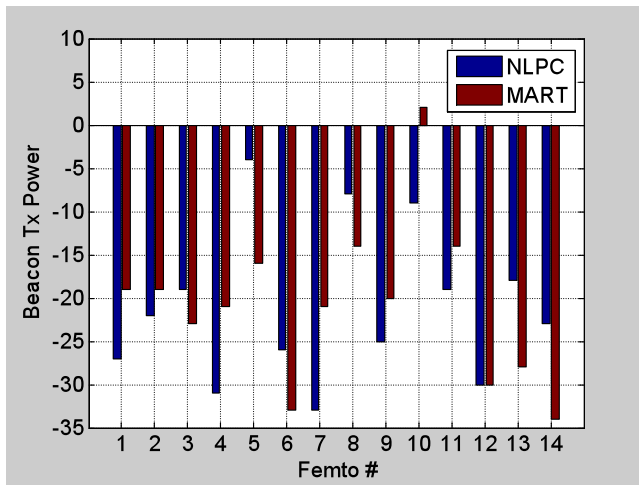


Figure 31: DUN beacon Tx power values for NLPC vs MART

Figure 32 shows the distribution of the number of registrations per day with NLPC versus MART. A value of 75dB is used for the PL_{edge} parameter in equation (3), and $E_{cp/Ior} = -3dB$, when computing the initial NLPC power values. Notice that after 14 days of MART the number of registrations per femto is tightly concentrated. Contrast this with NLPC, for which some femtocells receive hundreds of unique user registrations per day.

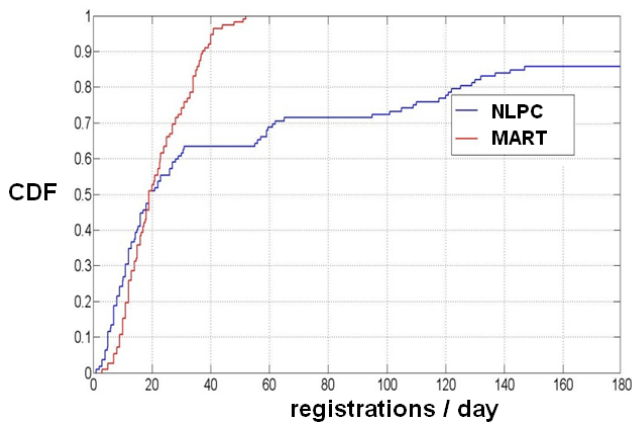


Figure 32: Distribution of # registrations/day

Figure 33 and Figure 34 display the beacon coverage region in the DUN with the initial NLPC and final MART settings, respectively. This is the region in which beacon $E_{cp/Io}$ is 3dB greater than the best macro $E_{cp/Io}$. In these figures we have only displayed the 1st floor of each apartment building, and the 7 femtocells located on this floor– the remaining 7 femtocells are present on higher floors, but we have excluded them from the figures for the sake of visual clarity.

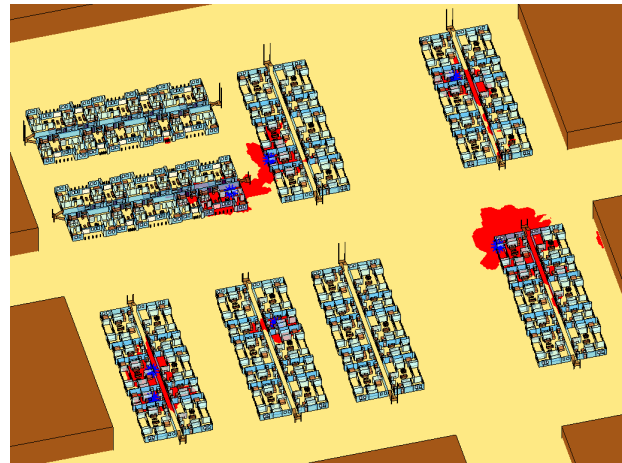


Figure 33: Beacon coverage in DUN for initial NLPC setting

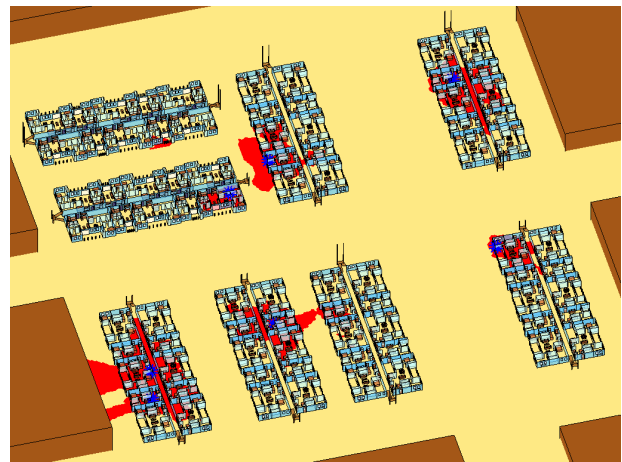


Figure 34: Beacon coverage in DUN after MART is run for 14 days

Notice from Figure 31 that the beacon Tx power sometimes increases after MART and sometimes decreases, depending on the femtocell location.

For instance, the beacon Tx power of femto #13 decreases from -18dBm to -28dBm after MART. This femto is located near a window facing the street, on the 1st floor of the bottom right building in Figure 33 (in the top left corner of the building). From the figure we see that the NLPC beacon spills out into the street and will potentially generate a substantial number of registrations from passing automobile traffic, and in particular from cars that stops at the intersection due to red lights (see Figure 25). Consequently we can see from Figure 34 that after MART is run, beacon coverage no longer extends out onto the street. This intuition is supported by Figure 35 which shows the number of registrations each day for this femto. On day 1 with the NLPC power setting there are 400 alien user registrations. By day 5 this has been brought down to the target level of 30. Figure 36 displays the corresponding power setting vs. day.

On the other hand, femtocells in out-of-the-way apartments such as the two, in the lower left apartment, experience an increase in beacon Tx power after MART (eg. femto #10). This is because few pedestrian or vehicular users pass within the vicinity of these femtocells. Consequently beacon coverage can be increased without substantially increasing the number of user registrations.

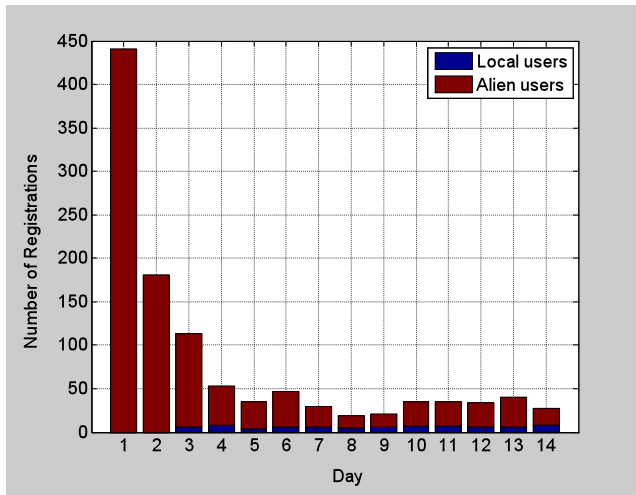


Figure 35: Illustration of MART. Number of registrations vs. day for femto located near street corner in DUN

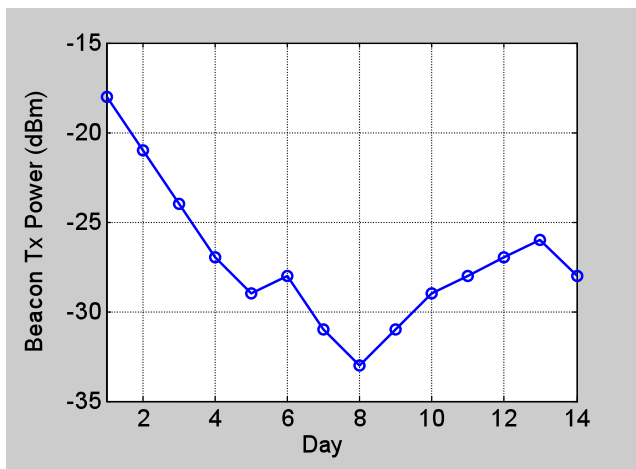


Figure 36: Illustration of MART. Beacon Tx power vs. day for same femto as Figure 35.

Similar results obtained for the SN are now briefly described. In this example the neighborhood is dropped at the *cell center* location of Figure 30. We first concentrate on the house in the lower left corner of the central T-intersection (see Figure 4), which we refer to as *house 1*. There is a femtocell in a bedroom on the second floor. Being close to the street, it initially experiences many registrations from passing users. As a consequence, beacon coverage shrinks due to MART. The initial NLPC power value is -2dBm and the corresponding beacon coverage on the first floor is displayed in red in Figure 37. The final MART power setting at the end of day 14 is -7dBm is displayed in green.

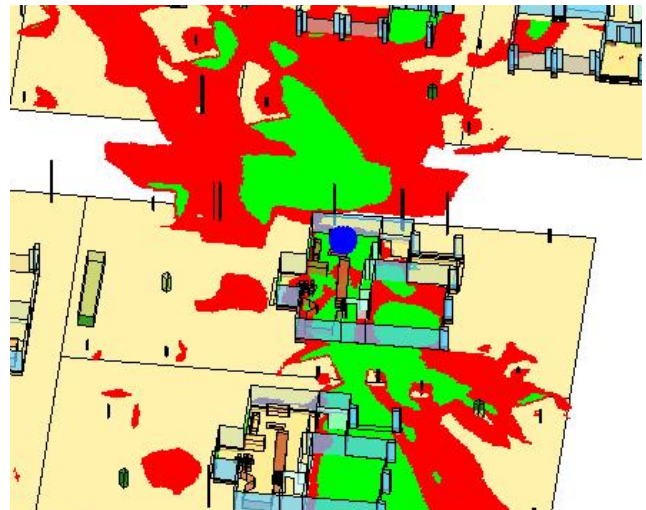


Figure 37: Beacon coverage for femto near street in SN. Initial NLPC setting (red) and final MART setting (green) after 14 days are shown.

In contrast we examine the house in the second row from the top, second from the left in Figure 4. There is a femtocell on the first floor in the back right. It is far from the street and consequently the MART algorithm behaves in the opposite manner— increasing beacon coverage, rather than decreasing it. Over 14 days the initial NLPC setting of -4dBm is raised to +5dBm. This is illustrated in Figure 38 where it can be seen that the initial setting in green spills onto the street, generating numerous registrations from passing users and neighbors, whereas in the final setting the beacon has been reigned in such that only the house itself is covered.

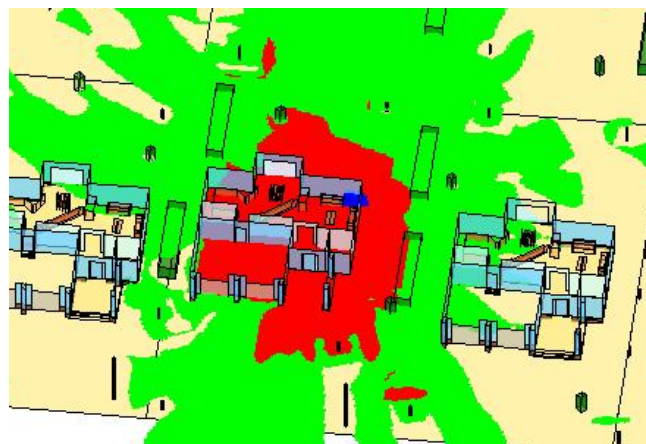


Figure 38: Beacon coverage for femto away from street in SN. Initial NLPC setting (red) and final MART setting (green) after 14 days are shown.

These examples serve to illustrate the efficacy of the MART algorithm in tailoring beacon range so as to facilitate discovery of the femtocell by a small number of local users, whilst preventing discovery of the femtocell by hordes of passing users. The backbones of our design and analysis are the DUN and SN RF models are the corresponding user mobility models.

6.2 Beacon Throttling

As discussed in section 6.1, if beacon Tx power is too high, active users served by the macro that walk or drive past the femto, will experience FL voice artifacts. Whilst the use of enhanced power calibration techniques such as MART goes a long way toward mitigating this effect, there are certain scenarios in which they will not be able to appropriately manage interference. For instance, if a macro access terminal (MAT) in a call walks into an apartment containing a femtocell, or walks along a corridor past an apartment in which there is a femtocell behind the corridor wall.

To combat this potential problem we use a technique called *beacon throttling*. The idea is that if the femtocell detects that the RSSI on the macro UL is unusually high, it is likely that there is an active MAT nearby and the femtocell should momentarily decrease its beacon Tx power to allow the MAT to continue its call uninterrupted.

We model an active MAT entering a building, walking up the stairs to the 3rd level, along the corridor to the end, and into its apartment. This is the scenario illustrated in Figure 23. Within its apartment it traverses one lap of the circuit route of Figure 24. There is a FAP located on the desk of the lower center apartment, behind the corridor wall. This is represented in Figure 23 by a solid blue disc. The apartment containing the FAP is separated from the apartment traversed by the active MAT, by a single 1 bedroom apartment.

The simulation is run at slot level with inner and outer power control loops modeled on both the UL and DL. Soft combining is modeled on the DL. On the UL soft combining between macro A and the co-located macros B & C is modeled with softer combining being modeled between co-located macros B & C. Single path Rician fading is added to PL traces with $K = 1.5$ (linear) used for femto fading and $K = 5.0$ used for macro fading. Log-normal UL/DL imbalance is added with a 3dB standard deviation between the two, and a 5.12 second de-correlation time. Voice activity is modeled according to MSO model IS-871 with 16 states modeling transitions between full, 1/2, 1/4 and 1/8 rate frames on both UL and DL.

We consider two neighborhood locations in the macro cell: cell corner and cell center, illustrated in Figure 30. For each neighborhood location we present 4 figures i) the DL PL traces from the three serving macro ATs to the active macro AT, and the DL PL trace from the FAP, ii) system performance with no beacon transmitted, iii) system performance with beacon transmitted at NLM power setting with no throttling, iv) system performance with beacon transmitted at NLM power setting and throttling enabled. For the illustrative purposes of this simulation we assume the beacon is transmitted continuously (ie. single macro carrier, no hopping) at the NLPC power setting given by equation (3) with $PL_{edge} = 75\text{dB}$.

6.2.1 Cell Corner Results

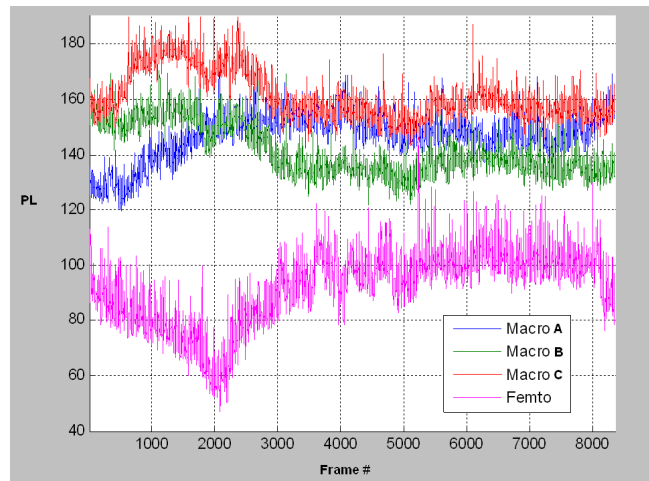


Figure 39: CELL CORNER. PL from MAPs and FAP to active MAT

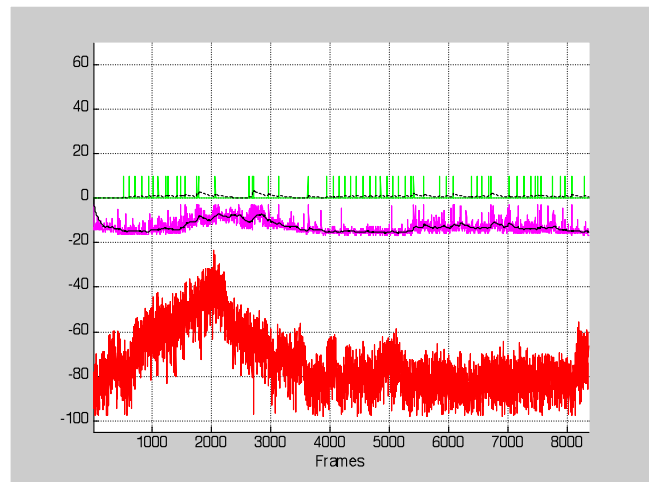


Figure 40: CELL CORNER. No Beacon

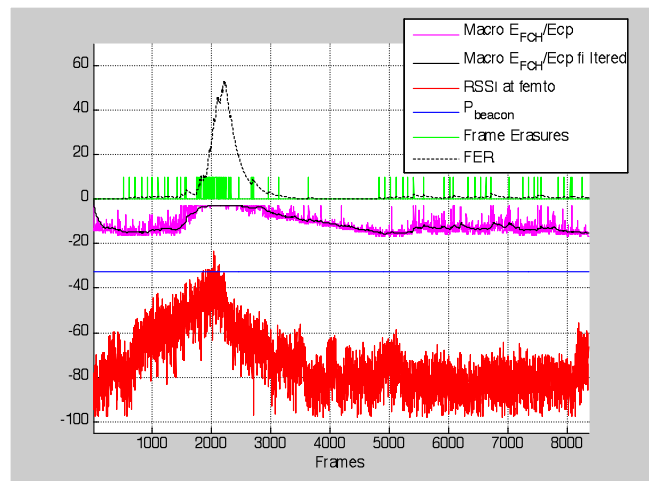


Figure 41: CELL CORNER. NLPC Beacon with no throttling

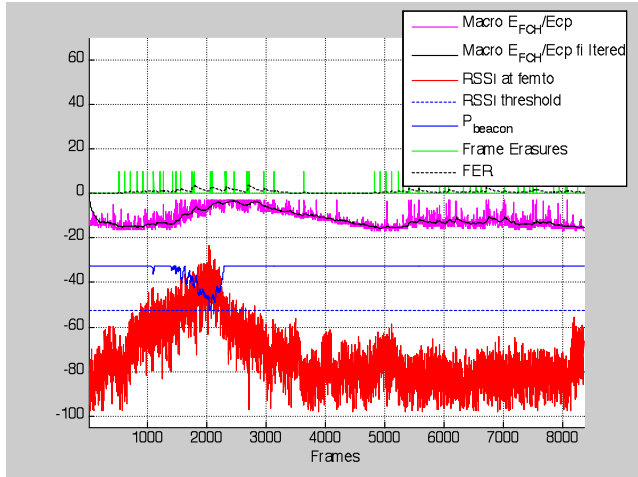


Figure 42: CELL CORNER. NLPC Beacon with throttling

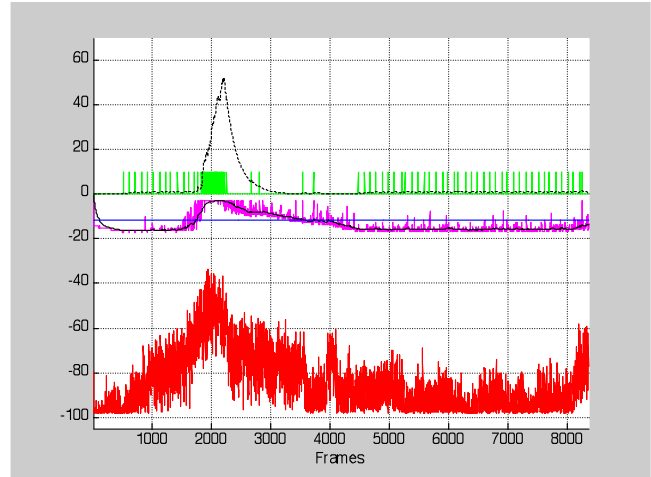


Figure 45: CELL CENTER. NLPC Beacon with no throttling

6.2.2 Cell center Results

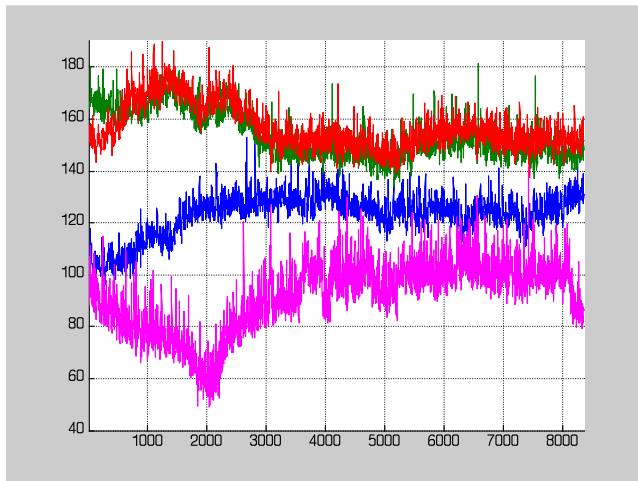


Figure 43: CELL CENTER. PL from MAPs and FAP to active MAT

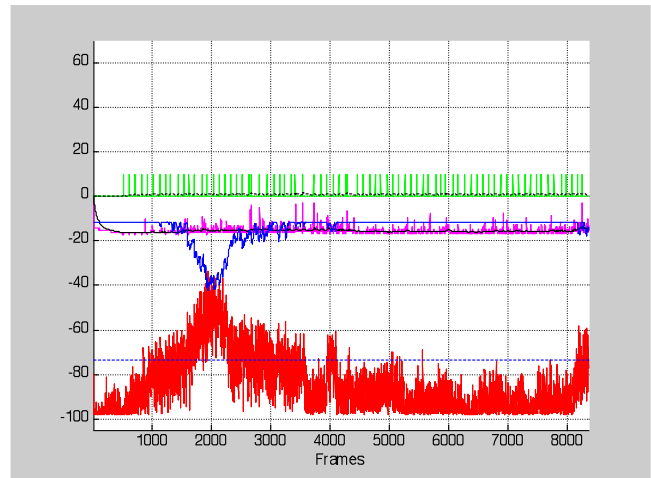


Figure 46: CELL CENTER. NLPC Beacon with throttling

The difference between the two cell locations should be clear from the PL traces. At cell corner the active macro AT hands off from macro A to macro B as it enters its apartment (approximately frame number 2000-3000), with macro A soon being dropped from the active set (Figure 39). At cell center, macros B & C never enter the ATs active set (Figure 43). It is evident from the traces that the user passes the FAP at approximately frame 2000 with the PL from MAT to FAP dropping to about 55dB (as the FAP is situated immediately behind the corridor wall).

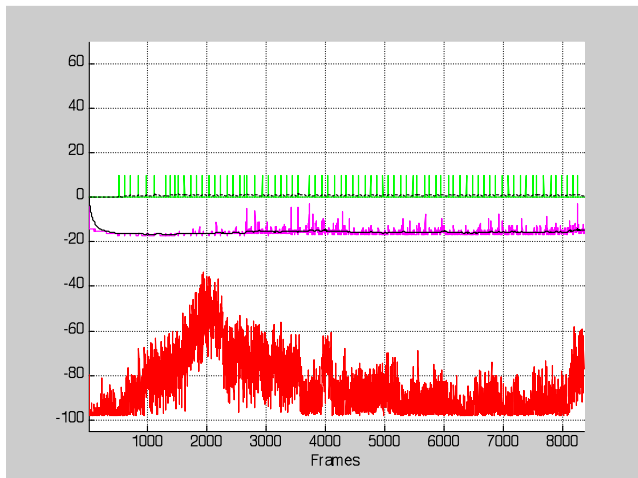


Figure 44: CELL CENTER. No Beacon

In the absence of beacon transmission, macro FCH allocation remains more or less constant throughout the MATs journey and the FER is maintained around 1% (Figure 40 and Figure 44). Notice that with beacon transmission but no throttling, the FCH allocation increases to maximum when the MAT passes the FAP and the FER rises to 30-50%, resulting in a stream of voice artifacts (Figure 41 and Figure 45). However when beacon throttling is enabled, we see that the beacon power drops in response to the increasing RSSI and the macro FCH allocation increases only slightly over the no beacon case (Figure 42 and Figure 46). Furthermore, the increase is more or less independent of the neighborhood location in the macrocell. Consequently the

MAT experiences very little impact as it passes by the femto, regardless of location in the macrocell.

This analysis thus supports our earlier claims that the femtocell can dynamically manage interference by throttling its beacon using RSSI measurements alone.

7. OTHER MODELS

In this section we give a brief overview of other RF propagation models we have developed using WinProp®.

7.1 Enterprise Campus

This is a model of an enterprise campus consisting of corporate office buildings. It is based on the Qualcomm Sorrento Valley campus with the main building modeled being QRC. Field measurements of a 1xRTT macro network and of femtocell signal strength were performed in and around this building. These were compared to a model created by importing the QRC CAD diagram into WinProp® and adding the exterior of the surrounding campus buildings (displayed in Figure 47).

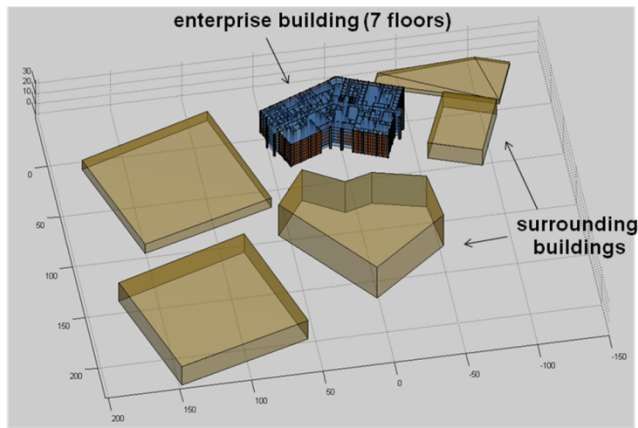


Figure 47: Enterprise Campus model

Figure 48 shows the agreement between PL measurements and WinProp® predictions for a scenario where there is a transmit antenna centrally located on the 1st floor of the building and an FFA on a cart is pushed at approximately constant speed through a series of corridors on the same floor.

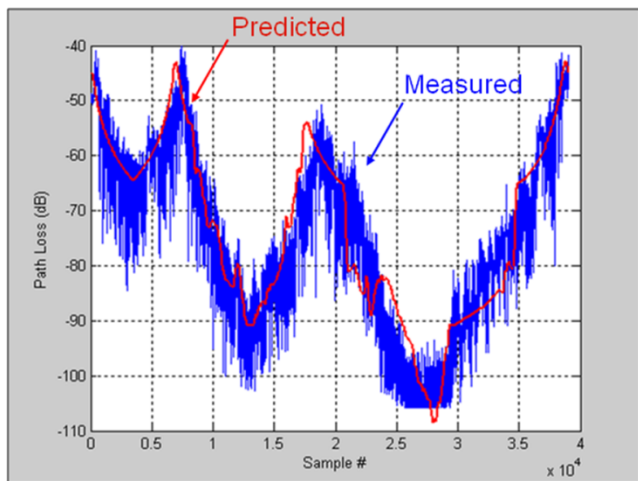


Figure 48: Agreement between indoor femto measurements and WinProp® prediction

Figure 49 shows the agreement between macro measurements and corresponding predictions. The methodology behind this comparison is as follows. A number of outdoor measurements were made (numbers 16,17 and 18 in Figure 49), in addition to the indoor measurements. In our model, the location of surrounding BSs is captured and each macro PL profile generated by WinProp® is offset by a constant amount so as to calibrate the data with outdoor measurements. The indoor predictions are thus *relative* to the outdoor measurements. The root mean square error of the indoor predictions is 2.3dBm.

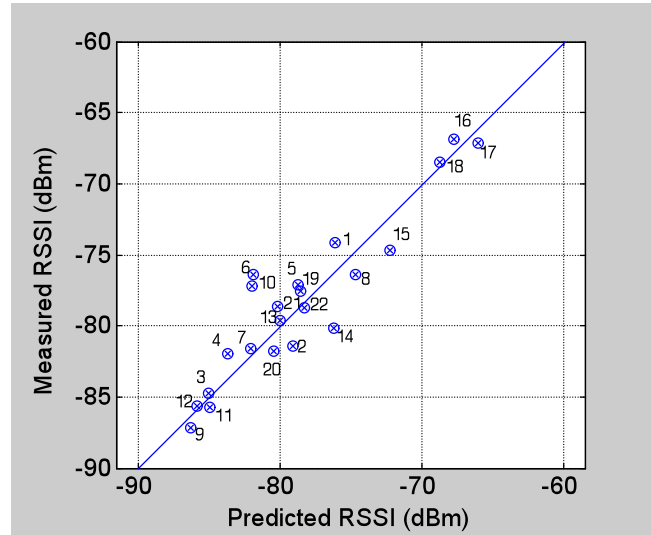


Figure 49: Agreement between macro measurements and WinProp® prediction

As a sample application of the enterprise model, we look at the problem of 1xRTT indoor beacon coverage for enterprise. For a large corporate office building such as QRC, the question arises as to how many femtos are required in order to provide adequate coverage. We have found that if deployed on a dedicated carrier, one 100mW (20dBm) femto is easily sufficient to provide coverage for a single floor, and if the building is located in a region where the macro signal (RSSI) is weak, one 100mW femto located on the center floor (number 4) can potentially provide coverage for the entire building. However a problem arises with femto discovery via beacon. The beacon must be transmitted on a macro carrier, and if the building is located in a region where the macro signal is strong, a 20dBm beacon may not be sufficiently powerful to enable the femto to be discovered by users at all locations on the floor. This is indeed the conclusion drawn based on our RF model as displayed in Figure 50. Here a 20dBm femtocell is centrally located in the building which is dropped at the cell center location of Figure 30. As is evident from the figure, the beacon is unable to facilitate discovery in certain regions of the floor near the corners.

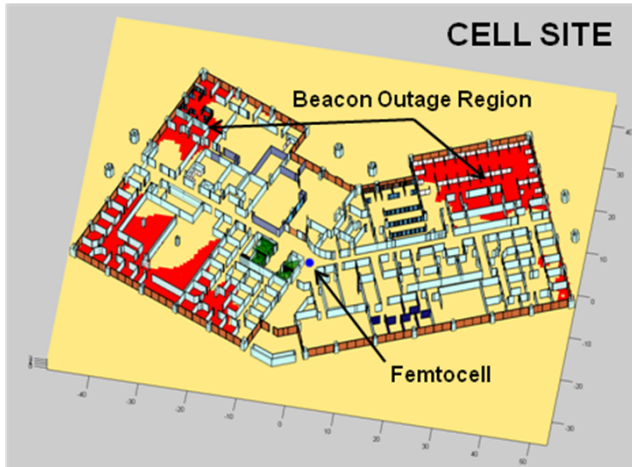


Figure 50: Beacon coverage in enterprise at cell center with 20dBm transmit power.

7.2 Big Box Store

This is a model of a large box like store such as Walmart or Best Buy, with 187,000 sq. ft. of floor space occupied by aisles, cloth stands, check-out counters, a customer-service area, offices, restrooms, etc... Depending on the number of channel elements per femtocell, it is possible that multiple femtocells will be required to provide adequate service with a low probability of call blocking. If multiple femtocells are deployed in the store in an adhoc manner some form of balancing may be required to evenly distribute the traffic load across the available resources. One way of achieving this is via power calibration. We use a model created in WinProp® to assess the efficacy of this approach. Three femtos are deployed. Femto 1 is attached to the center of the store ceiling (10m height). Femtos 2 and 3 are located in the corners of the store at 1.3m height. Figure 51 displays the coverage region of each femtocell when the pilot powers of all three femtos are set to 13dBm. The background RSSI level is -85dBm. It is clear that femto 1 will be forced to serve the bulk of the users in the store, making inefficient use of the channel elements available in corner femtos 2 and 3.

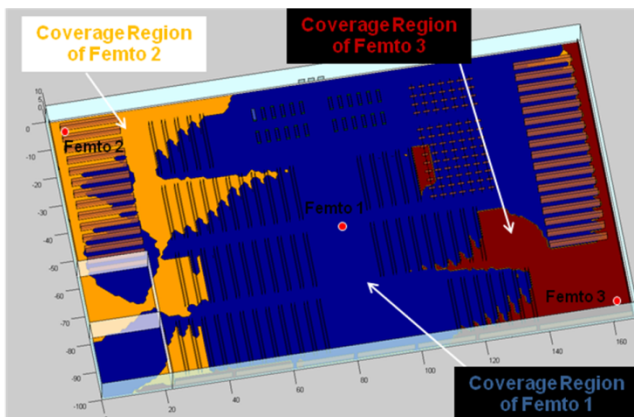


Figure 51: Femto coverage regions for big box store with no power calibration

Figure 52 displays the same scenario with femto power calibration. Here femtos 1, 2 and 3 transmit pilots with powers 4dBm, 10dBm, and 13dBm, respectively. The floor space covered

by each femto is now more evenly balanced and the load is likely to be more evenly distributed.

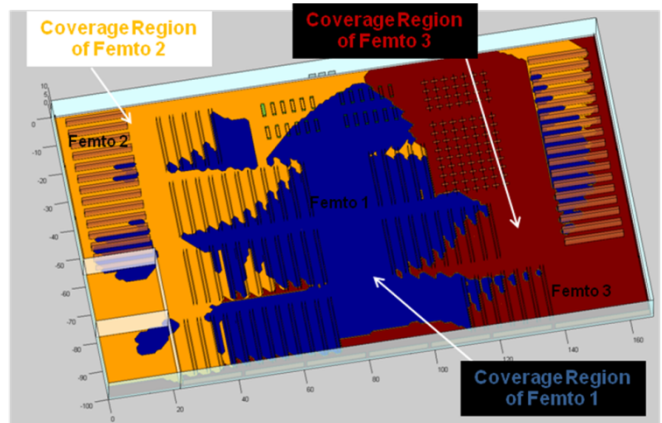


Figure 52: Femto coverage regions for big box store with power calibration

7.3 Large House

This is a model of a very large suburban home with approximately 6000 sq. ft. floor space, 3 floors of living space and over 20 rooms. A cut out of the first floor of the WinProp® model is displayed in Figure 53. The model is based on an actual residence in which measurements have been conducted. These were compared to the model predictions and found to be in close agreement. In the interest of brevity we omit further details.

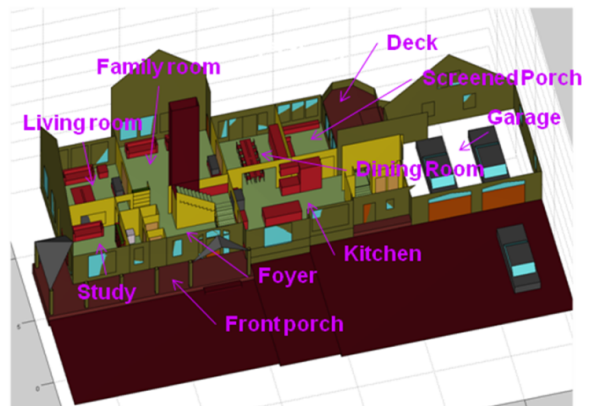


Figure 53: Large house model (first floor shown here)

To meet femtocell emission mask requirements we need to determine how much out-of-band attenuation the RF front end will have to provide. This requires that we first decide on the maximum Tx power required of the femtocell. The large house model represents one of the toughest foreseeable challenges in terms of required residential femtocell Tx power and for this reason we use it to determine the degree of coverage provided by different levels of Tx power. We place the femtocell in 10 different locations indicative of where it may be placed in practice. Figure 54 shows the fraction of the house in femto paging outage ($E_{cp}/I_o < -12\text{dB}$) as a function of Tx power for these 10 locations. The house is dropped in a region where the macro RSSI is high– the cell center location of Figure 30. From it we see that if the device is optimally placed it can cover 95% of the house with 10dBm. However, if our design goal is to provide

95% coverage regardless of femto placement, then up to 20dBm is required.

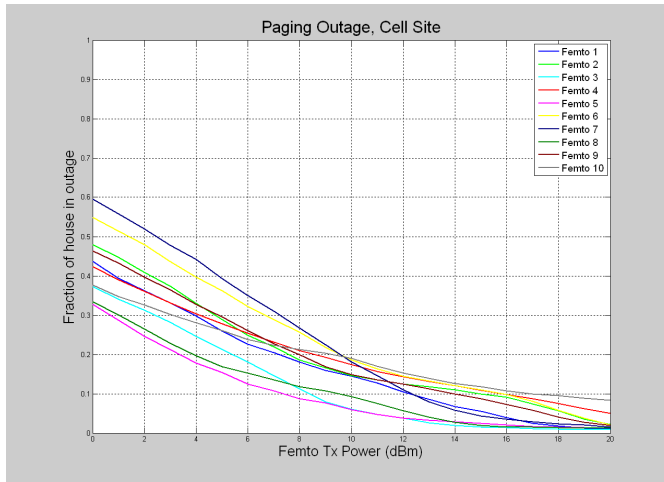


Figure 54: Paging outage as a function of femto Tx power, for different femtocell locations in the large house.

8. Conclusion

This paper has presented RF propagation models developed for urban femtocell environments using WinProp®. Field measurements have been used to verify the accuracy of models. Macro signal propagation is also captured and the environment can be dropped anywhere in the cell, to replicate the effects of being close to a site, or at the edge of several. We have primarily concentrated on the dense urban and suburban neighborhood models and demonstrated the high level of detail captured, by way of effects such as the gradation of macro RSSI with increasing floor in a mid-rise apartment building, and femtocell spillage onto the street when the device is placed near a window. A detailed user mobility model was created for both neighborhoods encompassing the movements of all users sampling every 1.28s continuously for 30 days. This model enabled us to design and simulate algorithms that rely on counting registration based events, such as Mobile Assisted Range Tuning. This application and others presented herein, demonstrate the great utility of these models in aiding the design and simulation of femtocell systems and algorithms.

9. References

- [1] Humblet P., et. al. "System design of cdma2000 femtocells," IEEE Comm. Magazine, vol. 47, pp. 92–100, Sep. 2009.
- [2] Yavuz M., et. al, "Interference Management and Performance Analysis of UMTS/HSPA+ Femtocells," IEEE Communications Magazine, pp. 102-109, Sept. 2009.
- [3] <http://www.awe-communications.com/>
- [4] Wölfle, Wahl Wertz, Wildbolz, and Landstorfer, "Dominant Path Prediction Model for Indoor Scenarios," German Microwave Conference, Ulm, 2005.
- [5] Patel C., et. al., "Femtocell and Beacon Transmit Power Self-Calibration," Qualcomm White Paper http://www.qualcomm.com/innovation/research/feature_project/femtocells.html